

Linear Angle Sensitive Pixels for 4D Light Field Capture

Vigil Varghese¹, Xinyuan Qian¹, Shoushun Chen¹ and Shen ZeXiang²

¹VIRTUS IC Design Centre of Excellence, School of Electrical and Electronic Engineering

²Division of Physics and Applied Physics, School of Physical and Mathematical Sciences

Nanyang Technological University, Singapore

Abstract—In this paper we present the design of an image sensor pixel which produces a linear response proportional to the incident light angle. Unlike conventional pixels, the proposed pixel encodes incident angles in terms of linear intensity variations. A set of four pixels can distinguish between incident light angles along both the vertical and horizontal directions. This coarse linear angle information can be combined with the precise non-linear Talbot effect based pixel response to deduce the exact incident angle. This technique greatly reduces the complexity of the Talbot effect based technique. Fabricated in a 65 nm GlobalFoundries mixed-signal CMOS process, the sensor can distinguish between angles in the range from -35° to $+35^\circ$.

Index Terms—Angle detection; image sensor; linear angle sensitive pixels.

I. INTRODUCTION

Light at a given point in space can be represented by an infinite collection of rays from all other points in space. This infinite collection of rays can be treated as a vector field, called the light field [1]. The Mathematical formulation of light field consists of a 7 dimensional function, called the plenoptic function [2]. The function (1) describes the light intensity at any point in space, at all times, for all wavelengths (color) and from all viewing directions. It comprises of the intensity along the two spatial directions x and y , along with the wavelength (λ), time (t) and the three viewing directions (V_x , V_y and V_z). For a motionless, monochromatic image this function becomes a 5 dimensional one, with x , y , V_x , V_y and V_z as the parameters.

$$P(x, y, \lambda, t, V_x, V_y, V_z) \quad (1)$$

Since it is impractical to sample this 5D function, a reduced 4D representation has been developed and used extensively [3][4]. This 4D representation provides a more complete description of the visual scene around us. Conventional image sensors can only capture a 2D version of the image scene and hence provide limited capabilities for post capture image enhancement. The complete 4D information allows for faithful 3D reconstruction [3][4][5] and post capture refocus [5].

There are several techniques to recreate a 4D light field using the direction of incoming light rays. Well known among them are the multi-aperture based and the Talbot effect based techniques. Multi-aperture based techniques [6] use an array of micro-lenses below the objective lens to capture the angle information. They require complex post processing and are

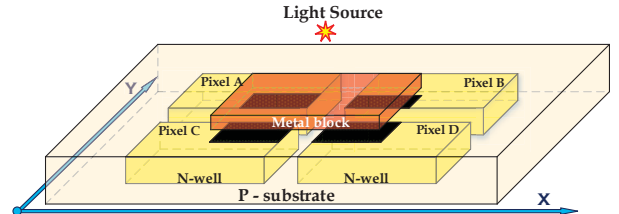


Fig. 1. Physical structure of a linear angle sensitive pixel.

computationally very intensive. On the other hand, Talbot effect based techniques [7][8] use on-chip diffraction gratings and have been touted as a suitable alternative for light angle capture. This technique is based on the microscale Talbot effect [9] and encodes angle information in terms of intensity. However, the response produced by pixels employing this technique is cosine in nature and a large number of pixels are required to faithfully estimate the angle information.

We propose a simple pixel structure - one that uses the metal shading principle [10] to capture the light angle. This technique takes advantage of the complementary response produced by a pair of adjacent photodiodes when they are partially shaded by a metal. The response produced by such an arrangement is linear in nature and in conjunction with the Talbot effect based pixels can reduce the complexity in determining the angles to a great extent.

The remainder of the paper is organized as follows: section II describes the principle behind the proposed method and verifies the claim through FDTD (Finite Difference Time Domain) simulations. Section III contains details regarding the sensor architecture and pixel design. Section IV illustrates the experimental results. Finally, we conclude by highlighting the main features of the proposed pixel type.

II. THEORETICAL DESCRIPTION AND SIMULATION RESULTS

The proposed linear angle sensitive pixel is based on the principle of metal shading, wherein a metal block is placed on top of adjacent photodiodes, which covers it partially. Fig. 1 shows the perspective view of such an arrangement containing four pixels. This simplified view shows four n-well/p-sub photodiodes with a metal block on top of them. The metal block is enclosed in the dielectric layer (not shown here for clarity). The diode pairs A/B or C/D give an indication of the angle variations along the horizontal (X) direction and

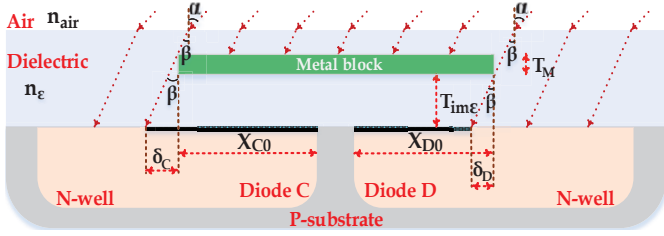


Fig. 2. 2D view of a linear angle sensitive pixel along the horizontal direction.

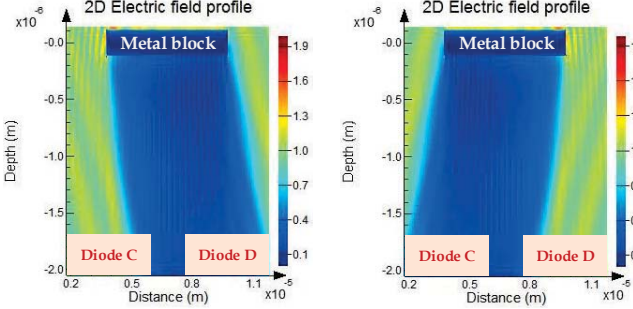


Fig. 3. FDTD simulations showing electric field profile for $\alpha = +40^\circ$ (left) and $\alpha = -40^\circ$ (right).

the diode pairs A/C or B/D give an indication of the angle variations along the vertical (Y) direction.

Fig. 2 shows the two dimensional view of a linear angle sensitive pixel along the horizontal direction. α and β are the incident and transmitted light angles at the air/dielectric interface. n_{air} and n_ϵ are the dielectric constants of air and dielectric respectively. X_{C0} and X_{D0} are the widths of the shaded regions of the diodes C and D at normal light incidence ($\alpha = 0^\circ$). δ_C and δ_D are the change in the widths of the shaded regions at non-normal light incidence ($-90^\circ \leq \alpha \leq +90^\circ$). Finally, T_M is the thickness of the metal block and $T_{\text{im}\epsilon}$ is the thickness of the inter-metal dielectric stack from the bottom of the metal block to the top of the photodiode surface.

From Snell's law we can write:

$$\beta = \arcsin\left(\left(\frac{n_{\text{air}}}{n_\epsilon}\right)\sin\alpha\right) \quad (2)$$

From Fig. 2, the change in the shading widths δ_C and δ_D over the diodes C and D can be written as:

$$\delta_C = (T_{\text{im}\epsilon} + T_M)\tan\beta \quad (3)$$

$$\delta_D = (T_{\text{im}\epsilon})\tan\beta \quad (4)$$

The response produced by a photodiode is proportional to the area exposed to the incident light. For non-normal light incidence, the area exposed to light will be different for different diodes because the metal block induces shadow over a small part of one diode whereas it exposes a small part of the other diode to light. This difference in the unshaded areas of the two diodes cause them to produce response proportional to the area exposed to light. FDTD simulations (Fig. 3) illustrate this concept more clearly.

Talbot effect based pixels employ a two level stacked diffraction grating (primary and secondary) to produce response proportional to the incidence angle. Since a particular

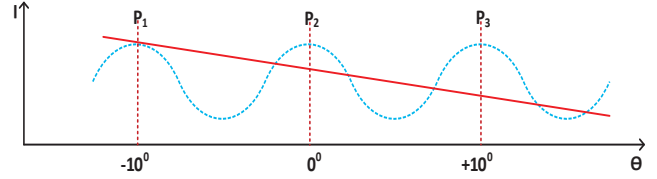


Fig. 4. Figure to illustrate coarse angle estimation and fine angle tuning.

grating orientation can detect angle variations only along a particular direction, two different grating orientations have been employed for bi-directional angle detection. According to the original design [7], a total of 32 pixels would be required for faithfully reproducing the angle information. 16 pixels each for the horizontal and vertical directions. These 16 pixels are divided into 4 groups of 4 pixels each. Each of the four groups have a different angular sensitivity.

The 4 pixels within any particular angular sensitivity group have their secondary grating offset from the primary by "0", "d/2", "d/4" and "3d/4", where "d" is the grating pitch. This is to avoid the dim-light-bright-light ambiguity (refer [7]) that is inherently present in the Talbot pixels. Angular sensitivity depends on the period of the harmonic cosine response produced by the Talbot pixels. Higher angular sensitivity means the range of resolvable angles is less and lower angular sensitivity means the difference in response produced by two adjacent angles is less. Hence the original design makes use of a set of 4 different angular sensitivity groups so as to resolve a wider range of angles.

By using the linear angle sensitive pixel (Fig. 1), we can greatly reduce the complexity of the Talbot effect based design. In this case, the need for 4 different angular sensitivity groups are eliminated, as the linear pixels provide a coarse angle estimation and the fine angle can be obtained from the Talbot pixels around the range of the coarse angle. Fig. 4 highlights this concept. The cosine curve is produced by a Talbot pixel. The linear curve is from a linear angle sensitive pixel. For example, if the angle of the incident light is $+2^\circ$, it would be impossible for a single Talbot pixel to determine the exact angle. We would require many different Talbot pixels, each with different angular sensitivities. Now, with a linear angle sensitive pixel, we can identify coarsely that the angle is around $+5^\circ$ (for example). Then we can choose the $P_2 - P_3$ segment of the Talbot response and accurately determine the fine angle. By having 2 Talbot pixel groups (horizontal and vertical Talbot pixels), and a linear angle sensitive pixel we can determine the light angle along both the vertical and horizontal directions. Hence, with a set of 13 pixels (one additional pixel for capturing raw intensity) we can accurately determine the angle variations compared to 32 pixels required by the actual microscale Talbot pixel design.

III. SENSOR ARCHITECTURE

The sensor was fabricated in 65 nm GlobalFoundries mixed-signal CMOS process and occupies an area of $1.6 \text{ mm} \times 1 \text{ mm}$. Fig. 5 shows the sensor architecture along with the chip microphotograph. The sensor contains a 12×10 array of macro-pixel clusters, each of which is made up of 4 macro-pixels. The 4 macro-pixels share a switched capacitor

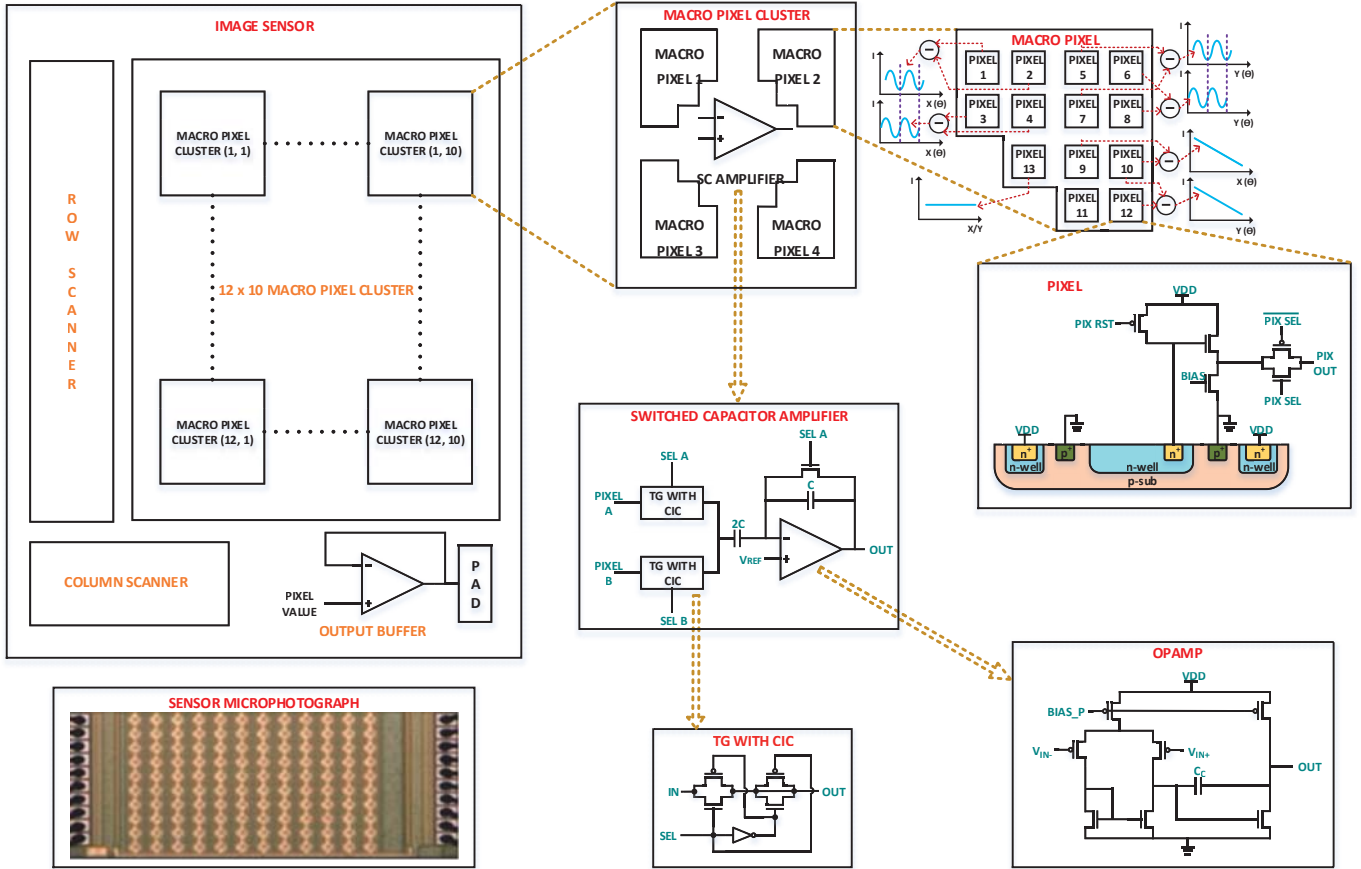


Fig. 5. Sensor architecture along with the chip microphotograph.

amplifier. The macro-pixels are in turn made up of 13 pixels each. All pixels share the same photodiode configuration and differ only in the type of metal structure above the photodiode. Each pixel is made up of a n-well/p-sub photodiode and 3 transistors, forming a conventional 3T pixel type. Additionally, the pixels have two more in-pixel transistors which are used for pixel selection. The photodiode is surrounded by a p+ guard ring and a n+ guard ring to isolate it from stray electrons and holes. The effective photo sensing area in each pixel is $6 \mu\text{m} \times 6 \mu\text{m}$ which gives a fill factor of 32% for a total pixel area of $12.5 \mu\text{m} \times 9 \mu\text{m}$.

Pixels 1 to 8 are Talbot pixels. Pixels 1 to 4 employ horizontal gratings and pixels 5 to 8 employ vertical gratings. The secondary grating of pixels 1 to 4 has an offset of 0, $d/2$, $d/4$ and $3d/4$ with respect to the primary. The same offsets apply to pixels 5 to 8. The difference response is taken between pixels 1, 2 and 3, 4 for horizontal direction and pixels 5, 7 and 6, 8 for vertical direction angle detection.

Pixels 9 to 12 contain a rectangular metal block on top of them and employ the differential metal shading technique to determine the light angle. Pixels 9 and 10 can determine angle variations along the horizontal direction and pixels 10 and 12 (or 9 and 11) can determine angle variations along the vertical direction. Pixel 13 does not contain any metal structure above the photodiode and is used to measure the raw intensity. Fig. 5 also shows the ideal response (Intensity, I) produced by each of the pixel types. In the ideal plots, $X(\theta)$ indicate angle variations along the horizontal direction

and $Y(\theta)$ indicate angle variations along the vertical direction.

The switched capacitor amplifier consists of a 7T opamp, two capacitors (C and $2C$) and two switches at the input. Output of the SC circuit is the amplified (by a factor of 2) difference of the two input signals. The output voltage is given by (5). Each input switch is made up of a transmission gate (TG) and two dummy transistors to cancel the charge injection (CIC) into the input capacitor when the transmission gate is turned off.

$$V_{\text{OUT}} = V_{\text{REF}} - \frac{2C}{C}(V_{\text{PIXELB}} - V_{\text{PIXELA}}) \quad (5)$$

IV. RESULTS AND DISCUSSION

The test setup for the experimental verification of the sensor consists of a sun simulator and a rotary board. The image sensor is mounted on a rotary board and is interfaced to the computer through the Opal Kelly XEM 3010 integration board. This setup is exposed to parallel rays of light from a sun simulator, which emits light over a broad spectral range (300 nm to 1000 nm).

Two sets of experiments were performed - one with a 500 nm optical filter over the sensor and the other without any filter. For each case the response was recorded by varying the angle of light incidence, first along the horizontal direction and then along the vertical direction. Fig. 6 and Fig. 8 show the voltage response produced by the horizontal Talbot effect based pixels (pixels 1, 2 and 3, 4) and the rectangular metal

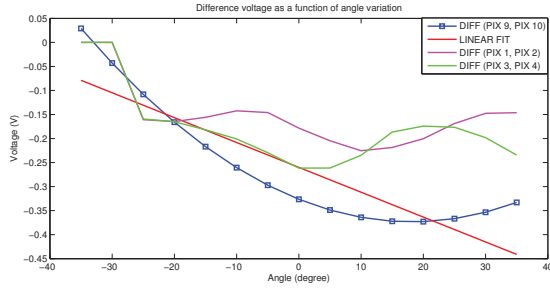


Fig. 6. Pixel response without filter (horizontal direction).

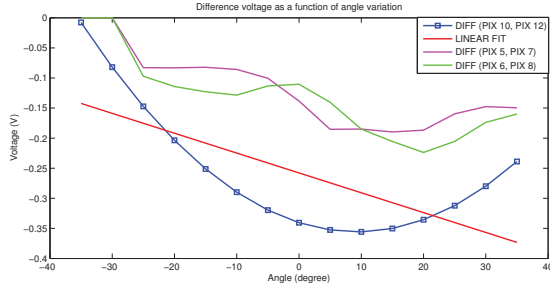


Fig. 7. Pixel response without filter (vertical direction).

shading pixels (pixels 9, 10). Similarly, Fig. 7 and Fig. 9 show the voltage response produced by the vertical Talbot effect based pixels (pixels 5, 7 and 6, 8) and the rectangular metal shading pixels (pixels 10, 12). For rectangular metal shading pixels, the raw experimental values were subjected to a polynomial fit of degree 2 and it is this data that is plotted. The curve is parabolic in nature because of the refraction of light at multiple dielectric interfaces within the CMOS metal stack and can be corrected to a certain extent by using the raw intensity pixel (pixel 13) value. A linear fit line indicates the general linear nature of the response.

The two sets of responses - with and without filter, show that the strength of the response produced by the Talbot effect based pixels are dependent on the wavelength. For a broadband source, self images for each wavelength is formed at a certain characteristic depth and the final response is due to the combined effect of all the self images. As can be seen from the plots, the Talbot effect based pixels produce strong response around the design wavelength of 532 nm (Fig. 8 and Fig. 9) and the response is relatively weak for a broadband source (Fig. 6 and Fig. 7). The rectangular metal shading pixels on the other hand produce an appreciably strong response at all wavelengths.

Since natural light contains a mixture of wavelengths, it is not feasible to design a sensor containing only Talbot pixels for angle determination. The pixels will exhibit large deviations in the strength of response and a large number of angular sensitivity pixel groups would be required for angle determination. On the other hand, since the response of linear pixels do not vary much with wavelength, it can still be used for coarse angle detection. Once the coarse angle has been determined, the Talbot pixels can then be used for fine angle determination.

V. CONCLUSION

In this paper we have presented a new pixel structure capable of detecting light angles along both the horizontal

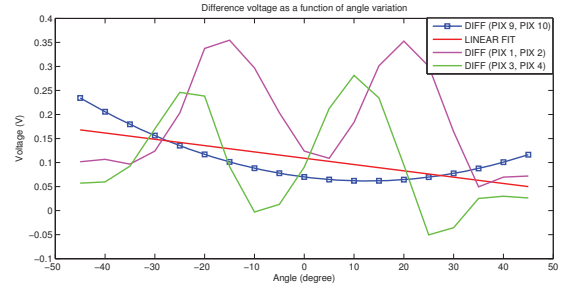


Fig. 8. Pixel response with 500 nm filter (horizontal direction).

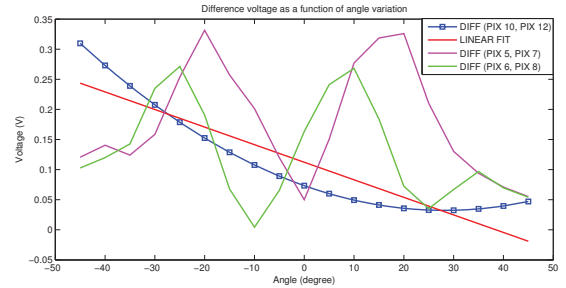


Fig. 9. Pixel response with 500 nm filter (vertical direction).

and vertical directions. The response produced by this pixel is linear in nature and is relatively independent of wavelength. The proposed structure can distinguish between angles over a broad range of 70° from -35° to $+35^\circ$. The sensitivity of response can be increased by using a higher metal layer compared to the one used in this design (metal 5). The main advantage of such a linear angle sensitive pixel is that it can be used in conjunction with the Talbot pixels to accurately determine the incident angles. As a result of this new passive angle detection technique we expect further advancement in the field of 3D image capture and object recognition.

REFERENCES

- [1] A. Gershun, "The light field," *J. Math. Phys.*, vol. 18, pp. 51–151, 1939.
- [2] E. H. Adelson and J. R. Bergen, "The plenoptic function and the elements of early vision," in *Computational Models of Visual Processing*. MIT Press, 1991, pp. 3–20.
- [3] M. Levoy and P. Hanrahan, "Light field rendering," in *Proceedings of the 23rd annual conference on Computer graphics and interactive techniques*, ser. SIGGRAPH '96. New York, NY, USA: ACM, 1996, pp. 31–42. [Online]. Available: <http://doi.acm.org/10.1145/237170.237199>
- [4] S. J. Gortler, R. Grzeszczuk, R. Szeliski, and M. F. Cohen, "The lumigraph," in *Proceedings of the 23rd annual conference on Computer graphics and interactive techniques*, ser. SIGGRAPH '96. New York, NY, USA: ACM, 1996, pp. 43–54. [Online]. Available: <http://doi.acm.org/10.1145/237170.237200>
- [5] K. Marwah, G. Wetzstein, Y. Bando, and R. Raskar, "Compressive Light Field Photography using Overcomplete Dictionaries and Optimized Projections," *ACM Trans. Graph. (Proc. SIGGRAPH)*, vol. 32, no. 4, pp. 1–11, 2013.
- [6] K. Fife, A. El Gamal, and H.-S. Wong, "A Multi-Aperture Image Sensor With $0.7\mu\text{m}$ Pixels in $0.11\mu\text{m}$ CMOS Technology," *Solid-State Circuits, IEEE Journal of*, vol. 43, no. 12, pp. 2990–3005, 2008.
- [7] A. Wang and A. Molnar, "A Light-Field Image Sensor in 180 nm CMOS," *Solid-State Circuits, IEEE Journal of*, vol. 47, no. 1, pp. 257–271, 2012.
- [8] A. Molnar and A. Wang, "Light field image sensor, method and applications," U.S. Patent US20110174998 A1, 07 21, 2011.
- [9] H. F. Talbot, "Facts relating to optical science. No. IV," *Philosoph. Mag.*, vol. 9, no. 56, pp. 401–407, 1836.
- [10] C. Koch, J. Oehm, and A. Gornik, "High precision optical angle measuring method applicable in standard CMOS technology," in *ESSCIRC, 2009. ESSCIRC '09. Proceedings of*, 2009, pp. 244–247.